Neuron
Article

Activity-Dependent Plasticity in an Olfactory Circuit

Silke Sachse,[1,4] Erroll Rueckert,[2] Andreas Keller,[1] Ryuichi Okada,[3,5] Nobuaki K. Tanaka,[3,6] Kei Ito,[3] and Leslie B. Vosshall[1,*]
[1]Laboratory of Neurogenetics and Behavior, The Rockefeller University, 1230 York Avenue, Box 63, New York, NY 10065, USA
[2]Department of Biochemistry and Molecular Biophysics and the Center for Neurobiology and Behavior, Howard Hughes Medical Institute, Columbia University College of Physicians and Surgeons, 701 West 168th Street, New York, NY 10032, USA
[3]Institute of Molecular and Cellular Biosciences, The University of Tokyo, 1-1-1 Yayoi, Bunkyo-ku, Tokyo 113-0032, Japan
[4]Present address: Max Planck Institute for Chemical Ecology, Department of Evolutionary Neuroethology, Hans-Knoell-Strasse 8, 07745 Jena, Germany.
[5]Present address: Laboratory of Functional Biology, Faculty of Pharmaceutical Sciences at Kagawa Campus, Tokushima Bunri University, 1314-1 Shido, Sanuki, Kagawa 769-2193, Japan.
[6]Present address: National Institute of Child Health and Human Development, 35 Lincoln Drive, MSC 3715, Bethesda, MD 20892, USA.
*Correspondence: leslie@mail.rockefeller.edu
DOI 10.1016/j.neuron.2007.10.035

SUMMARY

Olfactory sensory neurons (OSNs) form synapses with local interneurons and second-order projection neurons to form stereotyped olfactory glomeruli. This primary olfactory circuit is hard-wired through the action of genetic cues. We asked whether individual glomeruli have the capacity for stimulus-evoked plasticity by focusing on the carbon dioxide (CO_2) circuit in *Drosophila*. Specialized OSNs detect this gas and relay the information to a dedicated circuit in the brain. Prolonged exposure to CO_2 induced a reversible volume increase in the CO_2-specific glomerulus. OSNs showed neither altered morphology nor function after chronic exposure, but one class of inhibitory local interneurons showed significantly increased responses to CO_2. Two-photon imaging of the axon terminals of a single PN innervating the CO_2 glomerulus showed significantly decreased functional output following CO_2 exposure. Behavioral responses to CO_2 were also reduced after such exposure. We suggest that activity-dependent functional plasticity may be a general feature of the *Drosophila* olfactory system.

INTRODUCTION

In both mammals and insects, OSNs wire into the brain to form an intricate olfactory sensory map. A given olfactory glomerulus in the brain receives information from a subpopulation of OSNs expressing one or a few odorant receptors (ORs) (Couto et al., 2005; Fishilevich and Vosshall, 2005; Mombaerts et al., 1996; Ressler et al., 1994; Vassar et al., 1994). Odorants elicit the activation of specific subsets of glomeruli, producing a combinatorial neuronal odor code that has been proposed to form the basis of odor discrimination (Galizia et al., 1999; Johnson et al., 1998; Lin et al., 2006; Malnic et al., 1999 ; Wang et al., 2003). The map forms largely through the influence of hard-wired genetic cues, which in rodents includes the ORs themselves (Feinstein and Mombaerts, 2004), along with guidance and signaling molecules (Cutforth et al., 2003; Imai et al., 2006). In insects, olfactory map formation neither requires nor is influenced by OR expression (Ang et al., 2003; Dobritsa et al., 2003; Hummel et al., 2003; Hummel and Zipursky, 2004; Komiyama et al., 2004; Zhu et al., 2006; Zhu and Luo, 2004).

Once formed, the map—and the anatomical and functional properties of the neurons that compose the map—appears to be stable. When a subset of OSNs is ablated genetically in the mouse, the map is restored with complete fidelity over time (Gogos et al., 2000). The dendrites of individual identified mouse mitral/tufted neurons, which correspond to insect projection neurons, show remarkable neuroanatomical stability over a period of months, even under conditions of olfactory learning predicted to activate the olfactory subcircuit being examined (Mizrahi and Katz, 2003). In *Drosophila*, similar wiring stability has been documented. Ablation of sensory input in the adult has no effect on dendritic or axonal arborization of second-order projection neurons (Berdnik et al., 2006; Tanaka et al., 2004; Wong et al., 2002) or even on neurons in the secondary olfactory centers (Tanaka et al., 2004). The adult olfactory circuit thus respects the glomerular boundaries imposed during development.

Despite the stability of the overall map, the olfactory circuit appears to have the capacity for experience-dependent plasticity within the confines of a given glomerulus. In *Drosophila*, deprivation of input from one antenna reveals the existence of activity-dependent competition between the axons of ipsi- and contralateral OSNs in

a glomerulus (Berdnik et al., 2006). Olfactory learning in *Drosophila* modulates the physiology of glomerular circuitry on short time scales (Yu et al., 2004). In honeybee workers, the volume of a few identified glomeruli correlates with and is modulated by foraging experience outside the confines of the hive (Winnington et al., 1996). Previous studies in *Drosophila* showed that exposing flies to a single odor for several days causes stimulus-dependent decreases in glomerulus volume (Devaud et al., 2001, 2003). These earlier experiments by Devaud et al. were carried out before the odor tuning (Hallem and Carlson, 2006; Hallem et al., 2004) and molecular identity of individual olfactory glomeruli (Couto et al., 2005; Fishilevich and Vosshall, 2005) were available. We were interested in revisiting the question of glomerular plasticity in the *Drosophila* olfactory system but using odor ligands specific for identified circuit elements. To examine the neurophysiological and behavioral consequences accompanying stimulus-dependent anatomical plasticity within olfactory glomeruli, we focused on the dedicated circuit for CO_2 detection. CO_2 is a major component of *Drosophila* stress odor, which mediates potent avoidance behavior (Suh et al., 2004). In another context, CO_2 reduces attraction to food sources in female *Drosophila* (Faucher et al., 2006). In *Drosophila*, CO_2 is detected by a population of approximately 25–30 OSNs in the antenna that express the chemosensory receptor *Gr21a* (de Bruyne et al., 2001; Suh et al., 2004), which along with *Gr63a* comprises the *Drosophila* CO_2 receptor (Jones et al., 2007; Kwon et al., 2007). These OSNs project axons that terminate in the V glomerulus in the ventral antennal lobe (Scott et al., 2001). The *Drosophila* CO_2 circuit is ideal for studying odor-evoked plasticity because *Gr21a*-expressing OSNs are the only neurons in the fly that respond to CO_2 (Suh et al., 2004), and they do not respond to any other stimuli (de Bruyne et al., 2001). In this work, we examined stimulus-evoked changes in the anatomy and function of the *Drosophila* CO_2 circuit. The results provide functional evidence that a primary olfactory center is capable of activity-dependent plasticity.

RESULTS

CO_2-Specific Modulation of V Glomerulus Volume

We exposed newly emerged flies to elevated CO_2 levels and examined the antennal lobe for evidence of morphological plasticity. A given antennal lobe glomerulus is composed of processes from three different neuronal cell types: OSN axons, processes of inhibitory and excitatory local interneurons (LNs), and dendrites of projection neurons (PNs), which relay olfactory information to higher brain centers (Vosshall and Stocker, 2007). We wished to examine volume changes in the V glomerulus by selective visualization of OSNs and PNs with cell type-specific genetic markers. We therefore labeled OSNs that project to the V glomerulus with the *Gr21a*-Gal4 line. To visualize PNs that project dendrites into the V glomerulus, we used the Gal4-PN(V) enhancer trap line, which labels a single PN that selectively innervates the V glomerulus (N.K.T. and K.I., unpublished data). Flies carrying these cell type-specific Gal4 transgenes along with a UAS-GFP marker transgene were collected on the first day after adult eclosion and incubated either in ambient CO_2 (air; 0.04%) or elevated CO_2 (5%) for four days. Animals were sacrificed on the fifth day and their brains were processed for immunostaining and volumetric analysis of defined antennal lobe glomeruli, using the boundaries of GFP staining as a marker (Figure 1A). CO_2 exposure produced a mean 38% increase in the volume of the V glomerulus, both when measured with the fluorescent GFP tracer expressed in the axon termini of 25–30 OSNs (Figure 1B) or in the dendrites of one V glomerulus PN (Figure 1C). This increase was seen in both male and female flies.

CO_2 exposure had no effect on glomeruli that do not receive input from CO_2-sensitive OSNs. We measured the DA4 glomerulus, which receives input from *Or43a*-expressing OSNs tuned to cyclohexanol (Stortkuhl and Kettler, 2001) and other alcohols (Hallem and Carlson, 2006), and found no effect of CO_2 exposure on the DA4 glomerulus volume in male or female flies (Figure 1D). Similarly, the volume of the DM2 glomerulus, which receives input from *Or22a*-expressing OSNs that respond to esters and alcohols (Hallem and Carlson, 2006; Pelz et al., 2006), was unchanged after CO_2 exposure (Figure 1E). Because the absolute volume of the V glomerulus fluctuated across populations of flies reared in different vials at different times, our experiments were carefully controlled (see Experimental Procedures). This fluctuation precludes the comparison of absolute V glomerulus volumes across different experiments. Despite this variability, CO_2-induced V glomerulus volume increases were highly significant even when all measurements from all manipulations in Figures 1B and 1C and Figure 2B were pooled and analyzed ($p < 0.001$; see Figure S1 available online), demonstrating that activity-dependent volume increases were considerably larger than sample-to-sample variability. The volume effect was apparent in both sexes. We therefore carried out further glomerular volume experiments in male flies only.

Volume Increases Are Reversible and Occur in a Critical Developmental Window

We investigated the time course, reversibility, and sensitive period for volume increases induced by CO_2 in the V glomerulus. Flies were exposed either to 5% CO_2 or air for variable periods of time and analyzed at various time points (schematized in Figure 2A). We found that the volume increase required at least two days of exposure, as a single day of exposure showed no effect, and that volume was not further increased by a more prolonged 6 day exposure (Figure 2B). The effect was fully reversible, with V glomerulus volume restored to control levels 5 days after return to ambient conditions (Figure 2C, left). The time course of reversibility appeared to match that of the volume increase, because glomerular volumes returned to control levels as early as two days after return to

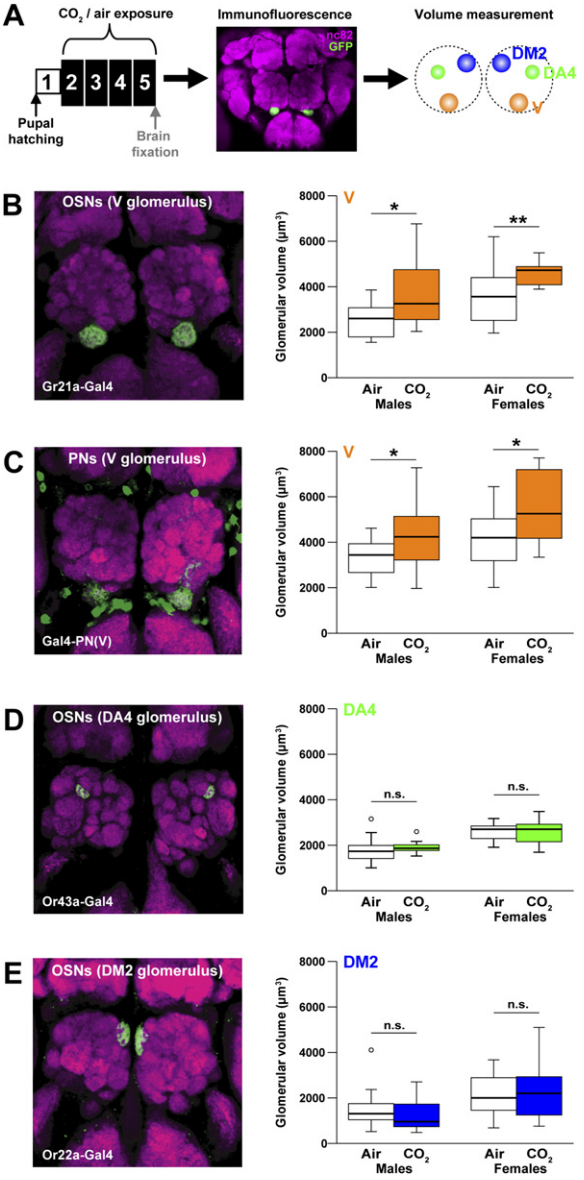

Figure 1. CO_2 Exposure Produces a Selective Increase in V Glomerulus Volume

(A) Schematic of experimental protocol used throughout this work, indicating that one-day-old flies (white box) were collected and incubated either in air or 5% CO_2 (black boxes) for the indicated number of days. Animals were analyzed at the time point indicated by the gray arrow (here at the end of the fifth day). Brains were dissected, stained with the general neuropil marker nc82 (magenta) and anti-GFP (green), and the indicated glomeruli were reconstructed from confocal images for volume measurement.

(B–E) Volume changes were measured in the indicated glomeruli, with an image of a fly brain expressing the indicated marker at left and box plots representing volume measurement at the right. The box plots here and in Figure 2 represent the median value (horizontal line inside the box), the interquartile range (height of the box, 50% of the data are within this range), and the minimum and maximum value (whiskers) of each experimental group. Circles depict outliers with values that were more than 1.5 times the interquartile range from the lower or upper quartile. The following markers were used to measure glomeruli: (B) *Gr21a* OSNs that project to the V glomerulus. (C) A single V-glomerulus PN labeled with Gal4-PN(V). Unrelated neurons are also labeled with this enhancer trap but were disregarded in the volume analysis. (D) *Or43a* OSNs that project to the DA4 glomerulus. (E) *Or22a* OSNs that project to the DM2 glomerulus.

Data from male (left) and female (right) flies were analyzed separately. Rearing conditions: air = ambient CO_2 (0.04%); CO_2 = 5%. V glomerulus volume was significantly increased by CO_2 exposure, while the volume of DA4 and DM2 remained unchanged (*$p < 0.05$, **$p < 0.01$, n.s. = not significantly different, unpaired, two-tailed t test). Fly genotypes and number of animals: *Gr21a*-Gal4; UAS-nsyb-GFP, n = 10-15 (A and B); Gal4-PN(V); UAS-nsyb-GFP, n = 10–21 (C); *Or43a*-Gal4; UAS-nsyb-GFP, n = 11–16 (D); *Or22a*-Gal4; UAS-nsyb-GFP, n = 14–20 (E).

ambient air (data not shown). The V glomerulus in flies 11 days posteclosion did not show exposure-induced plasticity in volume (Figure 2C, right).

Ligand-Specificity and Activity-Dependent Modulation of Glomerulus Volume

The volume increase of the V glomerulus was elicited specifically by CO_2 exposure. When flies were exposed to a control odor, ethyl butyrate, the volume of the V glomerulus was unchanged (Figure 2D). As expected, the same ethyl butyrate exposure produced a specific volume increase in the ethyl butyrate-sensitive DM2 glomerulus (Figure 2D). Therefore, stimulus-evoked plasticity of glomerular volume appears to be a general feature of the *Drosophila* olfactory system, as previously reported (Devaud et al., 2001, 2003).

To explore the mechanisms by which CO_2 modulates the volume of the V glomerulus, we asked whether odor-evoked activity in OSNs was sufficient to produce these neuroanatomical changes. This was achieved by ectopic expression and activation of an odorant receptor tuned to cyclohexanol in *Gr21a* neurons. Flies that express both *Or43a* and *Or83b* in *Gr21a* OSNs (*Or43a*/*Or83b*→*Gr21a*) were constructed as previously described (Benton et al., 2006; Figure 2E, top). In control experiments we monitored activation of the V glomerulus with the genetically encoded calcium sensor, G-CaMP (Nakai et al., 2001), in control and *Or43a*/*Or83b*→*Gr21a* flies (Figure 2E, bottom). We verified that cyclohexanol did not activate the V glomerulus in control flies (Figure 2E, bottom left) but that robust calcium release was evoked in the V glomerulus of *Or43a*/*Or83b*→*Gr21a* animals (Figure 2E, bottom right). Both control and *Or43a*/*Or83b*→*Gr21a* flies were then exposed to cyclohexanol for 4 days, using the same protocol as for CO_2 exposure (Figure 1A). V glomerulus volume in control flies was unaffected by this manipulation (Figure 2F, left), but in *Or43a*/*Or83b*→*Gr21a* flies, cyclohexanol induced a significant volume increase in the V glomerulus (Figure 2F, right). We conclude that neuronal activity in the OSNs is sufficient to induce neuroanatomical modulation of the V glomerulus. This experiment also allows us to exclude the possibility that the CO_2-evoked volume increases are merely a trivial effect of hypoxia rather than stimulus-evoked neuronal activity.

Sensory Exposure Produces Neither Morphological nor Functional Changes in Gr21a OSNs

We next asked whether CO_2 exposure evokes an increase in V glomerulus volume by increasing the number of *Gr21a*-expressing neurons or the morphology of axonal arborization. The number of *Gr21a*-GFP labeled neurons in antennae from air and CO_2-exposed flies was quantified (Figure S2A) and no significant differences were found (Figure S2B). The terminal axonal arbors of single *Gr21a*-expressing neurons obtained by the FLP-out technique (Wong et al., 2002; Figures S2C and S2D) were reconstructed in three dimensions (Figure S2D) and the number of branches, total length, surface, and volume were quantified (Figure S2E). No significant differences were found in any of these parameters. Therefore, the volume increase found for the V glomerulus cannot be explained by morphological change in the OSNs.

Although sensory exposure produced no morphological change in OSNs, we wondered if the physiology of these neurons is altered by prolonged exposure to CO_2. Functional imaging of the terminals of *Gr21a* neurons in the V glomerulus with G-CaMP was used to measure CO_2-evoked responses in air- and CO_2-exposed flies (Figure 3A). Representative images show basal G-CaMP fluorescence in the V glomerulus (Figure 3B, top left). CO_2-free air produced no increase in fluorescence over background, but even ambient air containing 0.04% CO_2 induced an increase in the intracellular calcium concentration (Figure 3B). Higher CO_2 concentrations evoked larger responses, with an apparent saturation in the response at 5%–10% CO_2 (Figure 3B). The temporal profile of these responses is shown in Figure 3C. CO_2-evoked calcium increases in the V glomerulus in CO_2-exposed flies were indistinguishable from air-exposed flies at all concentrations tested (Figure 3D). We conclude that the physiology of these neurons is not changed by sensory exposure at the level of resolution obtainable by calcium imaging.

Sensory Exposure Modulates Neuronal Activity of Local Interneurons

We reasoned that chronic stimulation of *Gr21a* neurons may produce functional effects in other neurons in the antennal lobe circuit. A network of GABAergic inhibitory LNs is thought to modulate odor-evoked activity in the *Drosophila* antennal lobe (Ng et al., 2002; Wilson and Laurent, 2005; Wilson et al., 2004). It seemed plausible that such neurons would exhibit anatomical or functional plasticity after CO_2 exposure. To investigate this, we examined whether odor exposure modulates the number of LNs in the antennal lobe. Two different Gal4 enhancer trap lines that label nonoverlapping GABAergic populations of LNs (Gal4-LN1, Gal4-LN2; R.O. and K.I., unpublished data) were used for this analysis. Both populations of LNs are multiglomerular and target all or most antennal lobe glomeruli. Gal4-LN1 labels a median of 18 LNs (range = 15–22; R.O. and K.I., unpublished data) and Gal4-LN2 labels a median of 37 LNs (range = 28–44; R.O. and K.I., unpublished data). We did not find any significant increase in LN number with either Gal4 line upon exposure to CO_2 (data not shown). We attempted to examine exposure-dependent changes of single LN clones, but even single neurons had such dense arborization within the V glomerulus that reconstructing and quantifying the branches proved to be technically impossible (data not shown).

To examine whether CO_2 exposure induces functional changes in either population of LNs, we used calcium imaging to measure CO_2-evoked responses in LN1 or LN2 arborization in the V glomerulus (Figure 4A). Gal4-LN1-labeled LNs project evenly across all antennal lobe glomeruli, with processes targeting the core of each glomerulus (Figure 4B). To locate the position of the V glomerulus for imaging, we used a V-RFP transgenic line (constructed by fusing the *Gr63a* promoter to n-synaptotagmin-RFP [*Gr63a*-nsyt-RFP] [Jones et al., 2007]) in concert with Gal4-LN1 and UAS-G-CaMP transgenes (Figure 4C). *Gr21a* and *Gr63a* are coexpressed in the CO_2-sensitive neurons that target the V glomerulus (Jones et al., 2007). Although CO_2 evokes calcium increases in LN processes in nearly all antennal lobe glomeruli, we quantified the levels only in the V glomerulus. Such global activation of LNs by a specific odor has been shown previously (Ng et al., 2002). Interestingly, we found that the LN1 population responds to CO_2 in a manner only weakly dependent on concentration (Figure 4D) compared to the strong dose dependence of *Gr21a* OSN activity (Figures 3C and 3D). There was no significant effect of CO_2 exposure on the CO_2-evoked (Figure 4E) or odor-evoked (Figure 4F) activity of the LN1 neurons in the V glomerulus.

We next examined the functional properties of a second population of LNs marked by Gal4-LN2. The processes of Gal4-LN2-expressing LNs appear to fill both the core and periphery of each glomerulus (Figure 4G). To measure CO_2-evoked responses in these neurons, we expressed G-CaMP in Gal4-LN2 in combination with the *Gr63a*-nsyt-RFP transgene to locate the position of the V glomerulus (Figure 4H). CO_2 elicited widespread activity in most antennal lobe glomeruli, but highest activity was seen in the V glomerulus region. Like LN1, the LN2 population showed weakly concentration-dependent responses to CO_2 (Figure 4I). We found a large effect of CO_2 exposure on the dose-response curve of the LN2 population, with a significant increase in responsivity to CO_2 in the V glomerulus ($p = 0.011$), which was most obvious for CO_2 concentrations at and above 0.5% (Figure 4J). This increased responsivity was specific for CO_2, as the LN2 neurons imaged in the V glomerulus showed the same response to a control odor (ethyl acetate) in both air- and CO_2-exposed flies (Figure 4K). To ask whether CO_2 exposure could have an effect on suppressing responses to ethyl acetate in other glomeruli, we analyzed the ethyl acetate responses of LN1 and LN2 in the DM2 glomerulus, which is responsive to this odor (Hallem and Carlson, 2006; Pelz et al., 2006), but did not find any effect (Figure S3). Therefore, physiological effects of CO_2 conditioning are highly

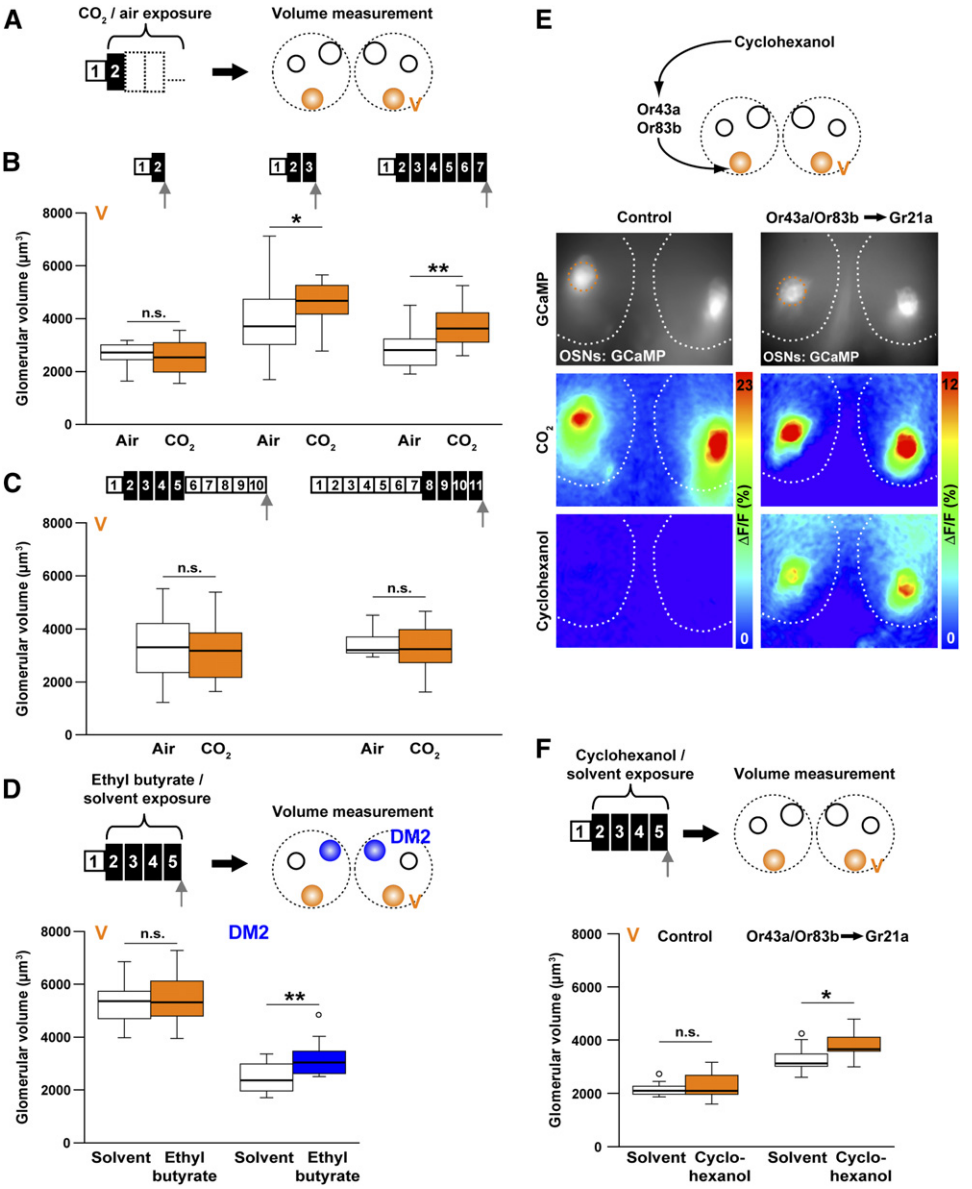

Figure 2. Volume Increases Occur and Are Reversible during a Critical Period

The effect is ligand- and glomerulus-specific and activity-dependent.

(A) Schematic of CO_2 exposure with varying numbers of days in ambient air (white boxes) and under CO_2 exposure (black boxes). Flies were collected on either the first ([B] and [C], left) or the seventh day ([C], right) after adult eclosion and the experiment was terminated on the day indicated by the gray arrow in the panels below.

(B) One day of CO_2 exposure (left) did not produce morphological change, while change was visible on the second day of exposure (middle) and did not increase with more prolonged exposure of 6 days (right). Conventions for the box plots are as described in legend to Figure 1.

(C) (Left) CO_2-evoked plasticity was reversible, with volume returning to control levels at 5 days (shown) and 2 days (data not shown) after return to ambient conditions. (Right) Volume increase to CO_2 did not occur in flies that were 7 days old at the beginning of exposure. For all panels: CO_2 concentration 5% compared to ambient air (0.04%). Fly genotype and number of animals: *Gr21a*-Gal4; UAS-nsyb-GFP, n = 12–20 flies per manipulation. Significance was assessed by unpaired, two-tailed t test. *$p < 0.05$; **$p < 0.01$.

(D) Ethyl butyrate exposure did not affect V glomerulus volume (white/orange box plot), but induced a selective volume increase of the DM2 glomerulus (white/blue box plot, **$p < 0.01$, unpaired, two-tailed t test). Odor concentration: 10^{-1} ethyl butyrate dissolved in paraffin oil, with paraffin oil as solvent control. Fly genotypes and number of animals: *Gr21a*-Gal4; UAS-nsyb-GFP (V glomerulus), n = 17–19 male flies; *Or22a*-Gal4; UAS-nsyb-GFP (DM2 glomerulus), n = 15 male flies. Experimental schematic and conventions for the box plots are as described in legend to Figure 1.

(E) Schematic of genetic manipulation to express Or43a and Or83b in Gr21a neurons (top). Functional calcium imaging of control flies (left) and flies with ectopic *Or43a*/*Or83b* expressed in the V-glomerulus OSNs (right). (Top) G-CaMP fluorescence image with V glomerulus outlined with orange dotted line; outlines of the antennal lobes are marked with white dotted lines. (Middle) CO_2 (5%) evoked calcium increase in both genotypes. (Bottom) cyclohexanol (10^{-2} in paraffin oil) evoked calcium increase only in *Or43a*/*Or83b*-ectopic animals. Fly genotypes: UAS-G-CaMP;*Gr21a*-Gal4 (control),

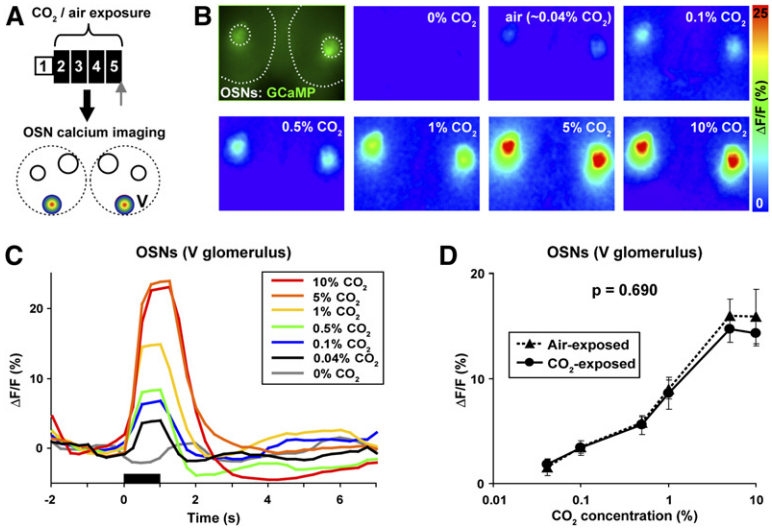

Figure 3. CO_2 Exposure Does Not Induce Functional Changes in Gr21a OSNs

(A) Schematic for measuring functional activation of *Gr21a* OSNs using G-CaMP.

(B) Intrinsic G-CaMP fluorescence (top left) and pseudocolor rendering of CO_2-evoked calcium release at a range of stimulus concentrations in a control fly. Frames are representative and show signal increase between frames 5 and 16 (before and at stimulus offset). Images represent ΔF/F (%) according to the scale at the right.

(C) Time traces of dose-dependent CO_2-evoked calcium increases from a representative animal.

(D) CO_2 exposure did not produce physiological changes in OSNs measured by calcium imaging. Peak evoked calcium values at a range of concentrations for control (triangle) and CO_2-exposed (circle) flies. Differences between these traces were not statistically significant ($p = 0.690$, repeated-measures ANOVA). Fly genotype: UAS-G-CaMP; *Gr21a*-Gal4; UAS-G-CaMP. Mean ± SEM, n = 4 flies per manipulation.

selective for the conditioning stimulus and the V glomerulus circuit.

CO_2 Exposure Reduces Projection Neuron Output in the Lateral Horn

To investigate whether the modulation of LN2 activity by CO_2 exposure alters the physiology of the PN innervating the V glomerulus, we used two-photon calcium imaging to examine functional activity in the single CO_2-sensitive PN labeled by the Gal4-PN(V) line. We measured calcium responses to CO_2 in the axonal terminals of this PN in the lateral horn of CO_2- and air-exposed flies (Figure 5A). A projection view of the basal G-CaMP fluorescence shows the complex axonal projection pattern of PN(V) in the lateral horn (Figure 5B). As has been shown for OSNs and LNs (Figures 3 and 4), CO_2-free air did not evoke any calcium activity over background, but increasing CO_2 concentrations induced strong and concentration-dependent calcium responses in axonal terminals (Figure 5C). The temporal profiles of these measurements are shown in Figure 5D. Interestingly, the PN-V showed strong concentration-dependency in contrast to the LN responses. In animals that have been exposed to CO_2 we found a significant reduction in the dose response curve to CO_2 compared to air-exposed flies (Figure 5E).

Sensory Exposure Selectively Reduces Behavioral Responses to CO_2

To determine whether the neuroanatomical and functional changes produced by CO_2 exposure affect behavioral responses to CO_2, we measured odor-evoked locomotor activity in an odor-flow assay (Keene et al., 2004; Keller and Vosshall, 2007). In this assay, an individual fly's position is monitored for 2 min in clean air and then 2 min in air supplemented with CO_2 or odor (Figure 6A). Behavioral responses were quantified as activity (distance walked per time) and showed a significant decrease in responsivity at and above 6% CO_2 in CO_2-exposed flies (Figures 6B–6D). Responses to a control odor (ethyl acetate) were not affected by CO_2 exposure (Figure 6E). Mirroring the reversibility of the V glomerulus volume increase, the decrease in behavioral responsivity to CO_2 was fully reversible, with behavioral responses returning to normal 5 days after a return to ambient CO_2 concentrations (Figure 6F). Finally, 11-day-old flies did not show behavioral plasticity in response to CO_2 exposure after the sensitive period surrounding early adult life (Figure 6G).

DISCUSSION

Taken together, our neuroanatomical, functional, and behavioral analysis suggests that the *Drosophila* olfactory system has the capacity for reversible activity-dependent plasticity. Evidence of this plasticity is readily seen by measuring the volume of the V glomerulus. Because the volume increase can be induced by odor activation of ORs ectopically expressed in the CO_2-activated OSNs, we conclude that persistent stimulus-evoked activity in these neurons underlies these anatomical changes. We and others have shown that stimulus-evoked plasticity is

UAS-G-CaMP/+;*Gr21a*-Gal4/UAS-GFP:*Or43a*;UAS-G-CaMP/UAS-*Or83b* (*Or43a-Gr21a*). GFP-tagged Or43a was restricted to cell body and dendrite, such that GFP fluorescence did not interfere with V glomerulus imaging.

(F) Cyclohexanol (10^{-2} in paraffin oil) induced specific volume increases in V glomerulus only in *Or43a*/*Or83b*-ectopic flies (*$p < 0.05$, unpaired, two-tailed t test). Fly genotypes and number of flies: *Gr21a*-Gal4; UAS-nsyb-GFP (control; n = 11 male flies); *Gr21a*-Gal4/UAS-GFP:*Or43a*;UAS-nsyb-GFP/UAS-*Or83b* (*Or43a*/*Or83b*→*Gr21a*; n = 9–10 male flies).

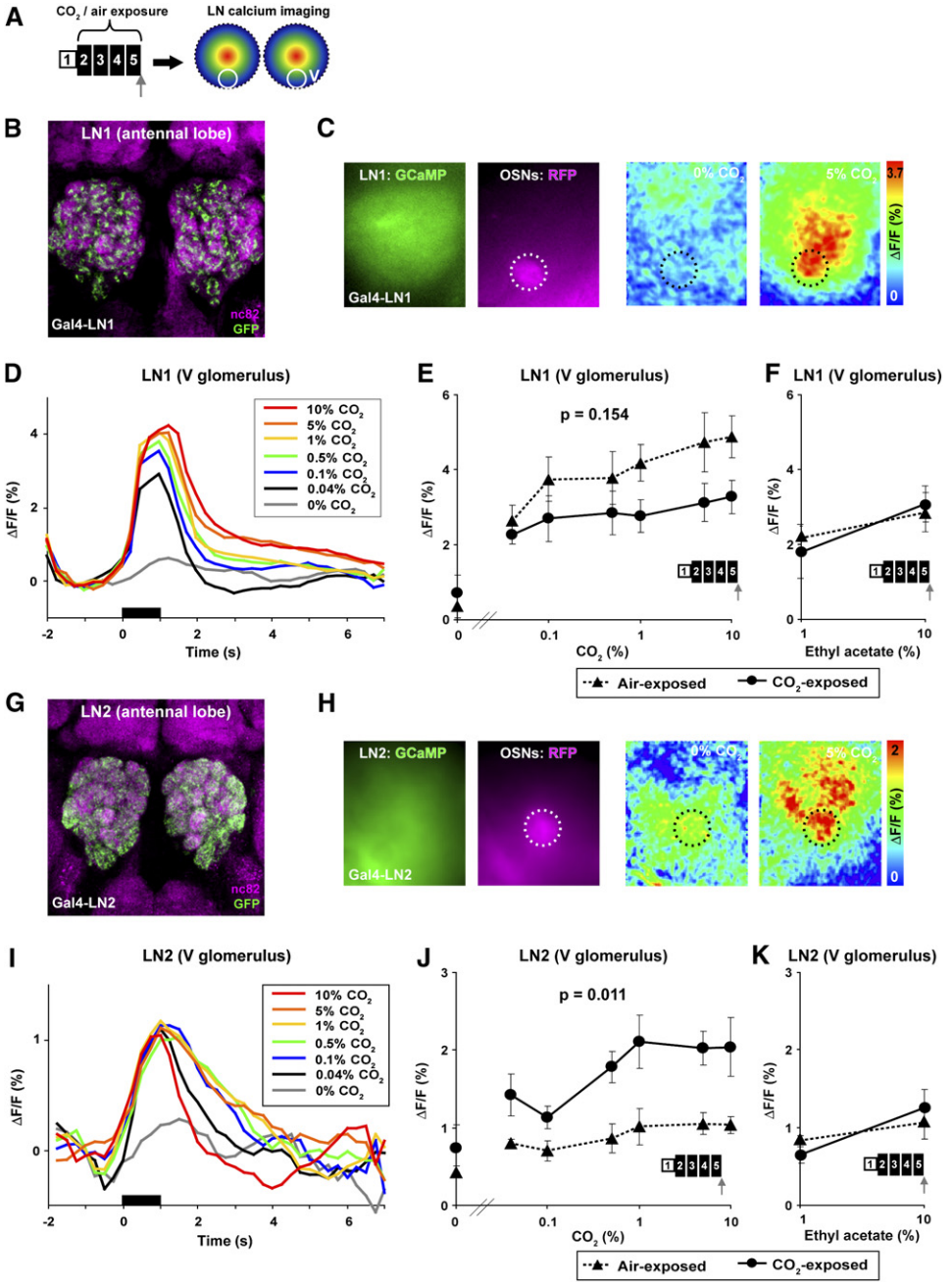

Figure 4. CO_2 Exposure Modulates CO_2-Evoked Responses in LNs

(A) Schematic for measuring functional activation of two different populations of LNs (LN1, [B]–[F] and LN2, [G]–[K]), using G-CaMP.

(B) Expression of Gal4-LN1 marker in adult antennal lobe. Staining: nc82 (magenta); anti-GFP (green). Neurons belonging to LN1 sparsely innervate the whole antennal lobe.

(C) Imaging LN1 neurons in the V-glomerulus assisted by a *Gr63a*-nsyt-RFP marker line that labels the V glomerulus (left panels). The V glomerulus is marked by the dotted circle. Five percent CO_2 evokes global calcium release throughout the antennal lobe (right panels), but we analyzed fluorescence only in the V glomerulus. Images represent ΔF/F (%) according to the scale at the right.

(D) Time traces of CO_2-evoked signals of LN1 innervating the V glomerulus in flies reared in air taken from a representative animal.

(E) Dose-response curves of CO_2-exposed and control flies at different CO_2 concentrations. CO_2-exposed flies show a trend toward decreased activity in LN1 neurons, which is not statistically significant ($p = 0.154$, repeated-measures ANOVA).

(F) LN1 responses to the control odor ethyl acetate are not affected by CO_2 exposure.

(G) Expression of Gal4-LN2 in the antennal lobe. Staining: nc82 (magenta); anti-GFP (green). LN2 neurons densely innervate all glomeruli of the antennal lobe.

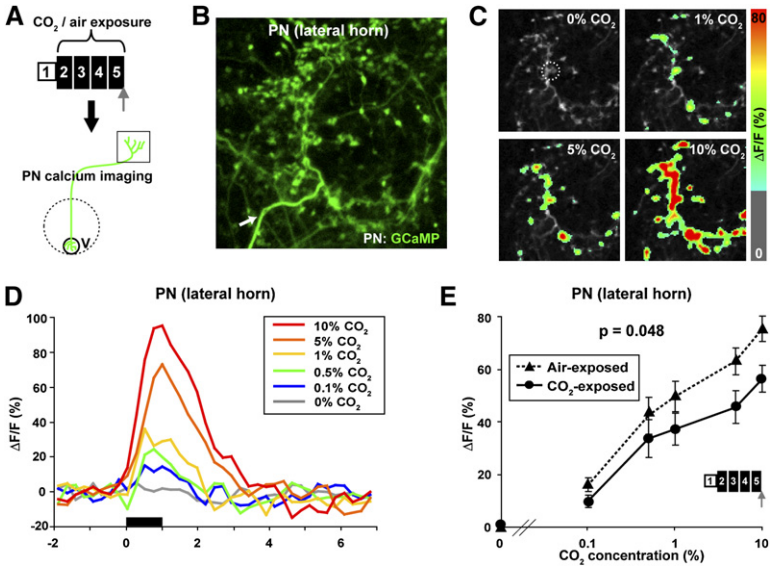

Figure 5. CO_2 Exposure Decreases CO_2-Evoked Output Responses in V Glomerulus PNs

(A) Schematic for measuring functional activation in the lateral horn of a single PN innervating the V glomerulus. G-CaMP was used as a genetically encoded calcium sensor. Imaging was done with a laser-scanning two-photon microscope.

(B) Intrinsic G-CaMP fluorescence of a single PN showing its axon terminals in the lateral horn. The axon, which projects from the V glomerulus, is marked with a white arrow.

(C) Pseudocolor rendering of CO_2-evoked calcium release in the lateral horn at a range of stimulus concentrations in a control fly. Frames are representative and show signal increase between frames 5 and 16 (before and at stimulus offset). Images represent ΔF/F (%) superimposed onto the raw fluorescence images according to the scale at the right.

(D) Time traces of dose-dependent CO_2-evoked calcium increases from a representative control animal of the region labeled by a white dotted circle in (C). Stimulation is given by the black bar.

(E) Dose-response curves of the PN to different CO_2 concentrations. CO_2 exposure leads to a significant decrease of the calcium activity in the lateral horn ($p = 0.048$, repeated-measures ANOVA). Mean ± SEM, n = 9 flies per manipulation.

Fly genotype: Gal4-PN(V); +; UAS-G-CaMP.

a general feature of the *Drosophila* olfactory system and not a peculiarity of the CO_2 circuit (Devaud et al., 2001, 2003). For instance, we find that the volume of DM2 is increased by chronic exposure to ethyl butyrate, a ligand for the *Or22a*-expressing neurons that target DM2.

Our data are consistent with a model in which one class of inhibitory LNs and the output of the V glomerulus are the major targets of plasticity induced by sensory exposure (Figure 7). Under conditions of ambient CO_2, the *Gr21a* circuit forms normally and small amounts of CO_2 produce robust behavioral responses. When flies are exposed to elevated CO_2 early in life, we postulate that chronic activation of *Gr21a* neurons promotes functional changes in the LN2 subtype of inhibitory local interneurons without affecting either the functional properties of the OSNs or the CO_2-evoked response of the LN1 neurons. We suggest that the volume increases seen with CO_2 exposure may result from neuroanatomical changes in the LNs, although their extensive glomerular arborization made this hypothesis difficult to test experimentally. Since a majority of the LN2 population in *Drosophila* has been shown to be GAD1 positive and thus to release GABA (Figure S4), as known for antennal lobe LNs in other insects (Christensen et al., 1998; Lei et al., 2002; Ng et al., 2002; Sachse and Galizia, 2002; Wilson and Laurent, 2005; Wilson et al., 2004), greater CO_2-evoked activity of LN2s may lead to an increased inhibition of the PN postsynaptic to *Gr21a* OSNs. Our finding of reduced activity in the output region of the PN innervating the V glomerulus supports this hypothesis. Thus, CO_2-evoked activity would be attenuated in the antennal lobe circuit in these animals, producing a corresponding decrease in the intensity of the behavioral response.

It has recently been shown that LNs are not only inhibitory, as has been assumed so far. A newly described population of excitatory cholinergic LNs forms a dense network of lateral excitatory connections between different glomeruli that may boost antennal lobe output (Olsen et al., 2007; Shang et al., 2007). Future studies are

(H) Calcium imaging of LN2 neurons in the V glomerulus using *Gr63a*-nsyt-RFP as a marker to label the V glomerulus (left panels). The V glomerulus is marked with a dotted circle. Five percent CO_2 stimulation leads to a strong widespread calcium increase with highest levels of calcium in the V region (right panels). Subsequent analysis of calcium responses was restricted only to the V glomerulus. Images represent ΔF/F (%) according to the scale at the right.

(I) Time traces of LN2 neurons to various CO_2 concentrations of a representative control animal.

(J) Dose-response curves of LN2 of CO_2-exposed and control flies. CO_2 exposure significantly increased the calcium activity of LN2 to different CO_2 concentrations ($p = 0.011$, repeated-measures ANOVA).

(K) CO_2 exposure did not affect calcium responses of LN2 to ethyl acetate.

Fly genotypes: UAS-G-CaMP/+; Gal4-LN1/CyO; UAS-G-CaMP/*Gr63a*-nsyt-RFP (B–F), Gal4-LN2/+; CyO/+; UAS-G-CaMP/*Gr63a*-nsyt-RFP (G–K). Differences in the relative amplitude of calcium signals in (D)–(F) and (I)–(K) are likely related to differences in G-CaMP copy number. Mean ± SEM, n = 5–7 flies per manipulation. The high resolution anatomical images in panels (B) and (G) were obtained with a Zeiss LSM510 confocal microscope, while the lower-resolution field of view images taken during calcium imaging were obtained at a fluorescence microscope with a CCD camera.

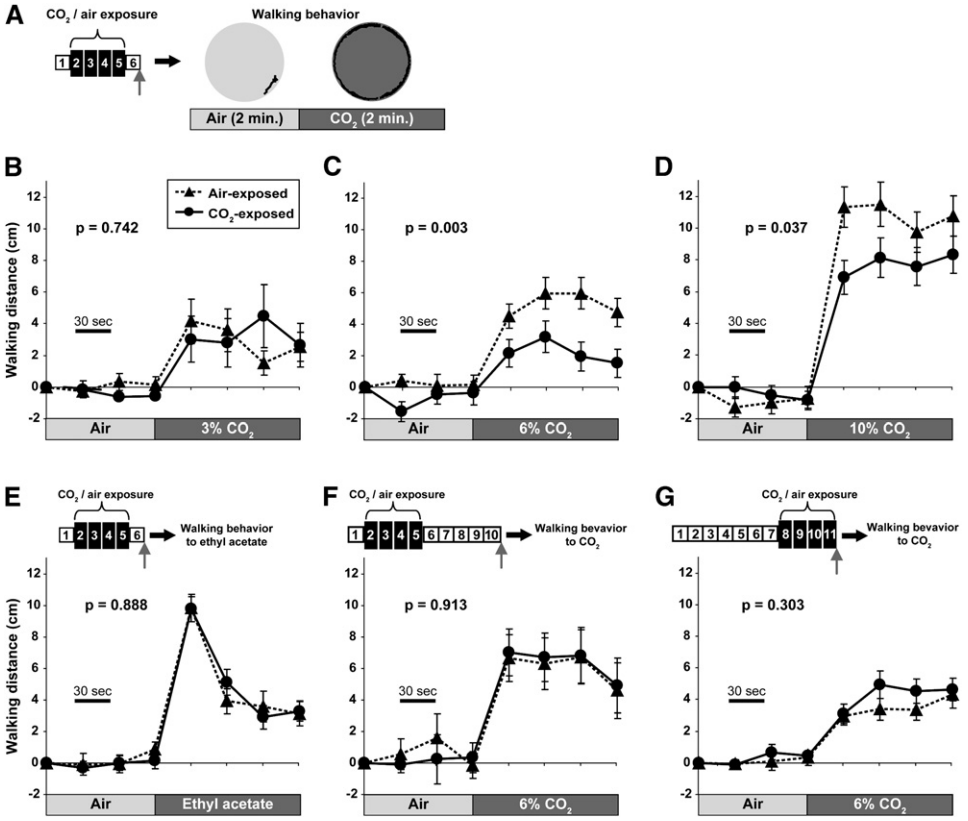

Figure 6. CO_2 Exposure Reduces Behavioral Responses to CO_2

(A) Odor flow assay schematic to analyze CO_2-evoked behavior after CO_2 or air exposure. Circles show example tracks of 4 min walking behavior (black trace) of a single fly during air for 2 min (bright gray arena) and subsequently during 10% CO_2 application for 2 min (dark gray arena).

(B, C, and D) Flies were exposed to either CO_2 or air for 4 days, and stimulus-evoked walking behavior was tested to different CO_2 concentrations (3%, 6%, or 10%) 1 day after the end of exposure. CO_2-exposed flies showed significantly reduced walking behavior to high CO_2 concentrations (C and D) compared to control flies (*$p < 0.05$, repeated-measures ANOVA). Genotype: wild-type Berlin. Mean ± SEM; (B) n = 24–50 flies, (C) n = 74–78 flies, (D) n = 106–114 flies.

(E) Behavioral response to ethyl acetate of flies that have been exposed to either CO_2 or air for 4 days. Ethyl acetate evoked a peak response followed by a strong decrease in walking behavior. CO_2 exposure did not affect behavioral responses to ethyl acetate ($p = 0.888$, repeated-measures ANOVA). Genotype: wild-type Berlin. Mean ± SEM, n = 85–89 flies.

(F) Walking behavior of flies tested 5 days after the end of CO_2 or air exposure. The reduction of the behavioral responsivity to CO_2 as shown in (C) and (D) was completely reversible ($p = 0.913$, repeated-measures ANOVA). Genotype: wild-type Berlin. Mean ± SEM, n = 30–31 flies.

(G) Behavioral response to CO_2 of flies that were 7 days old at the beginning of exposure. No significant effect of exposure was observed ($p = 0.303$, repeated-measures ANOVA). Genotype: wild-type Berlin. Mean ± SEM, n = 80–82 flies.

Data in (B)–(G) are binned, with each data point representing 30 s, such that the first four are before stimulus onset and the last four are after stimulus onset.

necessary to investigate if excitatory LNs are also subject to activity-dependent plasticity.

A Critical Period for Olfactory Plasticity in *Drosophila*

Stimulus-dependent plasticity can be induced and reversed in a critical period early in the life of a fly (Figures 2 and 6; Devaud et al., 2003). Similar critical periods have been documented in selective deafferentation periods in mammalian somatosensory and visual cortex. In all these model systems, the critical period likely allows the animal to compare the genetically determined network template with external conditions and make activity-dependent adjustments that reflect the external environment (Katz and Shatz, 1996). For instance, visual cortex "expects" binocular input when it is wired in utero. If monocular input is experimentally imposed, the system is rewired to reflect this (Hubel and Wiesel, 1962). The same rewiring occurs in the barrel cortex, in which the receptive fields of missing whiskers are invaded by neighboring whiskers, allowing the animal to maintain a continuous representation of external somatosensory space (Hickmott and Steen, 2005). *Drosophila* pupae have no sensory input during development and develop an olfactory system that relies neither on evoked activity nor the expression of ORs (Dobritsa et al., 2003; Elmore et al., 2003; Larsson et al., 2004). The time following adult eclosion may represent a period in which the functional set point of the *Drosophila* olfactory system is evaluated and adapted to the local environment.

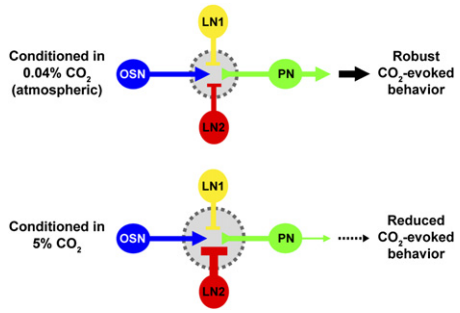

Figure 7. Model of Activity-Dependent Plasticity in the CO_2 Circuit

Schematic of the *Drosophila* CO_2 circuit, indicating putative functional changes elicited by CO_2 exposure. Exposing flies to different concentrations of CO_2 does not alter the functional properties of the *Gr21a*-expressing OSN (blue) or the LN1 class of local interneurons (yellow). However, inhibitory activity of the LN2 class of local interneuron is strongly increased (red) and CO_2-evoked activity of PN output neurons is strongly decreased (green), leading to the subsequent reduction in CO_2-evoked behavior.

Glomerular Volume Increase with Sensory Exposure

What elements of the antennal lobe circuit are responsible for the stimulus-dependent volume increases seen here? We were unable to find evidence that OSNs modulate their number, morphology, branching pattern, or functional properties in response to CO_2 exposure. The same neuroanatomical properties of single LNs or PNs could not be assayed due to the dense processes of these neurons in a given glomerulus. Since the observed net increase in volume cannot be ascribed to anatomical changes in OSNs, morphological plasticity is most likely occurring either at the level of LN or PN. We favor a model in which changes in the LNs underlie the observed volume increases because we find clear functional differences in LN2 responsivity in CO_2-exposed animals and because PN dendrites and axons have been shown by others to be extremely stable in size and morphology when deprived of OSN input (Berdnik et al., 2006; Tanaka et al., 2004; Wong et al., 2002). Similar stability in mitral/tufted cells has been shown in rodent olfactory bulb (Mizrahi and Katz, 2003). We cannot exclude the possibility that other cells, such as glia, contribute to these activity-dependent volume changes.

Two Functionally Distinct Classes of Inhibitory Local Interneurons

This work suggests that antennal lobe LNs marked with two different Gal4 enhancer traps, Gal4-LN1 and Gal4-LN2, are functionally distinct. The arborization of LN1 and LN2 processes in the V glomerulus suggests that they interact differentially with the antennal lobe circuitry. LN1 processes appear to innervate the core of a given glomerulus, while LN2 processes innervate the glomerulus more uniformly (Figure 4; R.O., N.K.T., and K.I., unpublished data). Both LN1 and LN2 neurons show weakly concentration-dependent tuning to odor stimuli. Thus, compared to the OSNs or PNs, which transmit a precise spike-timing code that reflects absolute CO_2 concentration, these LNs appear to respond in a binary fashion, showing similar levels of activity regardless of stimulus concentration.

There is a clear difference in how the responses of these two LN populations are modulated by CO_2 exposure. While the activity of LN1 neurons was not significantly affected by CO_2 exposure, LN2 neurons exhibited robust and significant increases in CO_2-evoked activity after CO_2 exposure. It will be of interest to examine the functional properties of these neurons in greater detail using electrophysiological approaches. It is plausible that circuit plasticity as evidenced in the LN2 neurons can be detected with electrophysiology at even lower CO_2 concentrations for shorter exposure periods.

Possible Neural Mechanisms of Odor-Evoked Plasticity

How might chronic activation of CO_2-sensitive OSNs specifically affect the physiology of LN2 neurons? We speculate that due to the broader innervation of LN2 processes, these neurons would receive greater presynaptic innervation from *Gr21a*-expressing OSNs. Thus, with chronic CO_2 exposure, the LN2 neurons would be chronically activated. This might cause long-term plasticity leading to greater GABA release from LN2 neurons. In cerebellar stellate cells, such an increase in inhibitory transmitter release has been documented and coined "inhibitory-long term potentiation" (I-LTP) (Liu and Lachamp, 2006). I-LTP is induced in stellate cells by glutamate released from parallel fibers acting on presynaptic NMDA receptors in these inhibitory interneurons and producing a long-lasting increase in the release of GABA from these cells (Liu and Lachamp, 2006). Like stellate neurons, at least one population of *Drosophila* LNs is pharmacologically GABAergic (Wilson and Laurent, 2005; Figure S4).

How might alterations in LN2 pharmacology affect downstream circuit elements and ultimately CO_2-evoked behavior? Drawing on the same cerebellar analogy discussed above, it is plausible that PNs exhibit a type of "rebound potentiation" that has been observed in Purkinje cells responding to inhibitory input (Kano et al., 1992). GABA released from LNs would regulate the excitability of PNs, such that greater GABA release from LN2 would tend to decrease the excitability of CO_2-specific PNs. Our finding that the output from the V glomerulus to the lateral horn is reduced following CO_2 exposure supports the idea that downstream activity in higher processing centers is modulated by the antennal lobe network. However, it still needs to be shown that LN2 neurons form direct inhibitory synapses onto PNs in the V glomerulus. Reduced PN activity in the lateral horn in turn may produce a reduced behavioral sensitivity to this stimulus. Future experiments that examine this stimulus-dependent plasticity at the cellular level using pharmacology and electrophysiology will be necessary to test this model.

EXPERIMENTAL PROCEDURES

Drosophila Stocks and Manipulations

All fly stocks were maintained on conventional cornmeal-agar-molasses medium under a 12 hr light:12 hr dark cycle at 18°C or 25°C. Transgenic lines used were as follows: *Gr21a-Gal4* (Scott et al., 2001); *Gr63a*-nsyt-RFP (Jones et al., 2007); *Or43a-Gal4* (Fishilevich and Vosshall, 2005); *Or22a-Gal4* (Vosshall et al., 2000); UAS-G-CaMP (Nakai et al., 2001; Wang et al., 2003); UAS-nsyb-GFP (Estes et al., 2000); UAS-GFP:*Or43a* (Benton et al., 2006); UAS-GFP:*Or83b* (Benton et al., 2006). The enhancer trap lines Gal4-PN(V), Gal4-LN1, Gal4-LN2 (R.O., N.K.T., and K.I., unpublished data) were provided by K.I. Specific genotypes are listed in the figure legends. *Gr21a*-FLP-out stocks were kindly provided by Allan Wong and Richard Axel (HS-FLP; UAS-FRT[CD2]FRT-CD8-GFP and UAS-G-CaMP). Single *Gr21a* OSN clones were made by heat shocking late-third-instar larvae (genotype, HS-FLP; *Gr21a*-Gal4; UAS-FRT[CD2]FRT-CD8-GFP) at 37°C for 10 min. The frequency of flies with single labeled neurons was ~6%.

CO_2 and Odor Exposure Protocol

Flies were exposed to an elevated CO_2 environment (5%) in a tissue culture incubator at 25°C for various days as indicated in the figures. Such sensory exposure did not affect the overall viability or fertility of flies, as assessed in early experiments in which flies were reared in these incubators for several generations. Control flies were reared at ambient CO_2 concentration (0.04%) and 25°C. Certified grade CO_2, diluted to 5% in air, was obtained from Matheson Tri-Gas (Parsippany, NJ).

For odor exposure experiments (Figure 2D), flies were exposed to a constant odor environment exactly as described (Devaud et al., 2001). In Figure 2F, we constructed a pulsed odor exposure protocol using solenoid valves (The Lee Company, Westbrook, CT) controlled by Programmable Logic Controllers (PLCs; powered by DirectSoft32 software; Automation Direct, Cumming, GA). This allowed us to expose flies to 30 s of cyclohexanol, followed by 5 min of clean air (1000 ml/min air flow). Odors were dissolved in paraffin oil (as indicated in the results) and were of highest purity available from Sigma-Aldrich (St. Louis, MO).

For all experiments, sibling flies reared from embryonic stages to adulthood in the same food vial were separated into control and experimental groups on the first day after adult eclosion. We noticed that V glomerulus volume varies between flies raised at different times in different vials. The basis for this variation is unknown. To control for this, all experiments in this study compared flies reared in the same vial divided at eclosion into control and experimental populations. However, when we averaged the absolute glomerular volumes of flies reared in different conditions and times of year the volume increase in the V glomerulus due to CO_2 exposure was highly significant (Figure S1).

Immunofluorescence

Whole-mount brain immunofluorescence staining was carried out essentially as described (Laissue et al., 1999; Vosshall et al., 2000), using these primary antibodies: nc82 (1:100; courtesy of Erich Buchner via Reinhard Stocker); rabbit polyclonal anti-GFP (1:1000; Molecular Probes, Carlsbad, CA). Secondary antibodies used were as follows: Alexa 488- and Cy3-conjugated anti-mouse IgG or anti-rabbit IgG 1:100 (Molecular Probes, Carlsbad, CA; Jackson ImmunoResearch, West Grove, PA). After mounting in Vectashield (Vector Labs, Burlingame, CA), images were collected with a Zeiss LSM510 confocal laser scanning microscope (Zeiss, Jena, Germany). Serial optical sections (512 × 512) were taken at 1μm intervals using a 40× water immersion lens. Antennal whole mounts of *Gr21a*-Gal4; UAS-GFP flies were stained with the GFP antibody (as described above). Confocal images of whole antennae were acquired as described above and the total number of labeled OSNs per antenna was quantified in the LSM Image Browser (Zeiss).

Volume Measurements

Three-dimensional confocal stacks were imported into the segmentation software Amira (Mercury Computer Systems, San Diego, CA). Using GFP staining, the glomerulus of interest was traced in every section for each confocal stack to reconstruct the glomerular structure and calculate its volume. In cases where the GFP staining was discontinuous, we extrapolated smooth lines to connect the boundaries of each glomerulus. Thus, blank areas devoid of staining are included in the final volume measurements. For each animal, left and right glomeruli were measured separately and averaged to produce a per-fly data point. Initially, male and female flies were analyzed separately. Odor and CO_2 exposure produced significant effects in both male and female flies (Figure 1), but most of our analysis was restricted to male flies (Figure 2). All confocal scans and reconstructions were carried out with the investigators blind with respect to the experimental treatment.

Optical Imaging

Imaging experiments were performed using female flies, because their bigger body size simplifies the dissection procedure. Flies were engineered to express the genetically encoded calcium sensor G-CaMP (Nakai et al., 2001; Wang et al., 2003) and were processed for optical imaging exactly as described (Benton et al., 2006). Flies were mounted such that the V glomerulus is imaged from a dorsal view, producing a different angle of view than the neuroanatomical analysis which was viewed frontally. For each measurement a series of 40 frames was taken at 4 Hz. CO_2 stimuli (1 s, i.e., frames 12–16) were puffed into a constant CO_2-free air stream (1000 ml/min) using a custom-made electronic valve under computer-control with a 1 min interstimulus interval. Imaging data were analyzed with custom-written IDL software (Research Systems) including noise filtering, movement and bleaching correction. Relative fluorescence changes (ΔF/F) were calculated by dividing the averaged fluorescence intensities from frames 4–6. False color-coded images (Figures 2–4) represent the signal increase between frames 5 and 16. For traces, 3 × 3 pixel squares were placed onto the center of the V glomerulus and the values averaged and plotted against time. For each fly, we calculated the stimulus response as the mean fluorescent change of frames 13–18 (Figures 3D, 4E, 4F, 4J, and 4K). Certified grade CO_2, diluted to various CO_2 concentrations in CO_2-free air was obtained from Matheson Tri-Gas.

Two-Photon Optical Imaging

An antennae-brain preparation was obtained by microdissection and embedded in 2% agarose with the antennae exposed to air (Wang et al., 2003). This preparation eliminates movement and allows for frontal viewing of the V glomerulus and PN axons. Images were acquired on a Prairie two-photon microscope using PrairieView acquisition software (Prairie Technologies, Middleton, WI). The light source was a Chameleon titanium:sapphire laser (Coherent, Santa Clara, CA) modelocked at a wavelength of 925 nm. The correct PN axon (innervating the V glomerulus) was identified by its distinctive morphology. For each measurement a series of 40 frames (128 × 128 pixels) was taken at 4 Hz. CO_2 stimuli (1 s, i.e., frames 12–16) were puffed into a constant CO_2-free air stream (400 ml/min). Data were analyzed with custom-written IDL software provided by Mathias Ditzen. Relative fluorescence changes (ΔF/F), false color-coded images, time traces, and mean fluorescent changes (Figures 5C–5E) were calculated as for the CCD imaging measurements.

Olfactory Behavior

Odor-flow behavioral experiments were carried out as described (Keene et al., 2004; Keller and Vosshall, 2007) using ethyl acetate (18% saturated vapor) and CO_2 (various concentrations diluted from 100% ultrapure CO_2 with filtered air). Single flies were placed into each of 16 circular arenas (10 cm diameter, 1 cm high, tilted walls) in a custom-built apparatus outfitted with individual odor intake and outlets and a Plexiglas lid to isolate flies in each arena. Flies were acclimated to a constant flow of pure air (590 ml/min) for 5 min. After

acclimation, flies were videotaped for the 6 min experiment, which consisted of 2 min exposure to flow of pure air and 4 min of subsequent exposure to air containing a given concentration of odor or CO_2. Only the first 2 min of odor or CO_2 application was analyzed, because walking responses decreased strongly during the remaining 2 min. Odorous air was produced by bubbling air through 100 ml of undiluted odorant in a gas washer and the odor rapidly equilibrated in the arena. The x-y position of the fly was tracked at 6 Hz using Ethovision (Noldus) and the walking behavior (distance walked/unit time) was calculated. Male and female flies were tested as mixed populations. The walking behavior data are normalized to zero at the beginning of the experiment. Therefore, if the flies are initially active and subsequently slow down, it is possible for walking behavior to result in values below zero.

Statistical Analysis

Data were analyzed for statistical significance using either unpaired two-tailed t tests for pairwise comparisons (Figure 1 and 2) or a two-way repeated-measures (RM) analysis of variance (ANOVA) for comparisons of repeated and dependent data sets (Figures 3–6) Throughout the paper, significance values are indicated as $^{*}p < 0.05$, $^{**}p < 0.01$, and $^{***}p < 0.001$.

Supplemental Data

The Supplemental Data for this article can be found online at http://www.neuron.org/cgi/content/full/56/5/838/DC1/.

ACKNOWLEDGMENTS

We thank Austen Gess, Ariana Andrei, Emily Cross, Avril Johnnidis, and Beate Eisermann for expert technical assistance; Mathias Ditzen for programming data analysis tools in IDL; Sonja Bisch-Knaden for statistical advice; Sabine Krofczik for help with neuronal reconstructions; Bill S. Hansson for providing support to S.S.; Geraldine Wright and Brian H. Smith for help with programming the PLC and building the pulsed-odor device; Randolf Menzel and Giovanni Galizia for providing support for optical recording of LNs; Maria Luisa Vasconcelos, Sandeep Robert Datta, Vanessa Ruta, and Anmo Kim for helpful technical advice regarding two-photon imaging of PN-V; Richard Axel for supporting the two-photon imaging experiments; Jean-Marc Devaud for fruitful discussions; and Giovanni Galizia, Kevin Lee, Kristin Scott, Marcus Stensmyr, Dieter Wicher, and members of the Vosshall laboratory for helpful comments on the manuscript. Pelin Cayirlioglu, Ilona Grunwald Kadow, and Larry Zipursky generously provided the *Gr63a*-nsyt-RFP fly line. Allan Wong and Richard Axel provided the strains for the FLP-out experiments. This work was supported by grants to L.B.V. from the NSF (IBN-0092693), the NIH (R01 DC05036), and the McKnight, Beckman, and John Merck Foundations. S.S. was supported by a Rockefeller University Presidential Postdoctoral Fellowship, and A.K. was supported by a Marco S. Stoffel Fellowship in Mind, Brain and Behavior. Further support was provided by a BIRD/JST grant and a Grant-in-Aid for Scientific Research from the Ministry of Education, Culture, Sports, Science, and Technology of Japan to K.I.

S.S. planned and carried out all the experiments in the paper with the exception of the behavioral experiments in Figure 6, which were performed by A.K., and the two-photon imaging experiments in Figure 5, which were performed with E.R.; N.K.T. characterized Gal4-PN(V); R.O. characterized Gal4-LN1 and Gal4-LN2; K.I. supervised N.K.T. and R.O.; S.S. and L.B.V. together conceived the experiments, interpreted the results, prepared the figures, and wrote the paper.

Received: October 27, 2006
Revised: July 30, 2007
Accepted: October 22, 2007
Published: December 5, 2007

REFERENCES

Ang, L.H., Kim, J., Stepensky, V., and Hing, H. (2003). Dock and Pak regulate olfactory axon pathfinding in *Drosophila*. Development *130*, 1307–1316.

Benton, R., Sachse, S., Michnick, S.W., and Vosshall, L.B. (2006). Atypical membrane topology and heteromeric function of *Drosophila* odorant receptors *in vivo*. PLoS Biol. *4*, e20. 10.1371/journal.pbio.0040020.

Berdnik, D., Chihara, T., Couto, A., and Luo, L. (2006). Wiring stability of the adult *Drosophila* olfactory circuit after lesion. J. Neurosci. *26*, 3367–3376.

Christensen, T.A., Waldrop, B.R., and Hildebrand, J.G. (1998). GABAergic mechanisms that shape the temporal response to odors in moth olfactory projection neurons. Ann. N Y Acad. Sci. *855*, 475–481.

Couto, A., Alenius, M., and Dickson, B.J. (2005). Molecular, anatomical, and functional organization of the *Drosophila* olfactory system. Curr. Biol. *15*, 1535–1547.

Cutforth, T., Moring, L., Mendelsohn, M., Nemes, A., Shah, N.M., Kim, M.M., Frisen, J., and Axel, R. (2003). Axonal ephrin-As and odorant receptors: Coordinate determination of the olfactory sensory map. Cell *114*, 311–322.

de Bruyne, M., Foster, K., and Carlson, J.R. (2001). Odor coding in the *Drosophila* antenna. Neuron *30*, 537–552.

Devaud, J.M., Acebes, A., and Ferrus, A. (2001). Odor exposure causes central adaptation and morphological changes in selected olfactory glomeruli in *Drosophila*. J. Neurosci. *21*, 6274–6282.

Devaud, J.M., Acebes, A., Ramaswami, M., and Ferrus, A. (2003). Structural and functional changes in the olfactory pathway of adult *Drosophila* take place at a critical age. J. Neurobiol. *56*, 13–23.

Dobritsa, A.A., van der Goes van Naters, W., Warr, C.G., Steinbrecht, R.A., and Carlson, J.R. (2003). Integrating the molecular and cellular basis of odor coding in the *Drosophila* antenna. Neuron *37*, 827–841.

Elmore, T., Ignell, R., Carlson, J.R., and Smith, D.P. (2003). Targeted mutation of a *Drosophila* odor receptor defines receptor requirement in a novel class of sensillum. J. Neurosci. *23*, 9906–9912.

Estes, P.E., Ho, G., Narayanan, R., and Ramaswami, M. (2000). Synaptic localization and restricted diffusion of a *Drosophila* neuronal synaptobrevin—green fluorescent protein chimera in vivo. J. Neurogenet. *13*, 233–255.

Faucher, C., Forstreuter, M., Hilker, M., and de Bruyne, M. (2006). Behavioral responses of *Drosophila* to biogenic levels of carbon dioxide depend on life-stage, sex and olfactory context. J. Exp. Biol. *209*, 2739–2748.

Feinstein, P., and Mombaerts, P. (2004). A contextual model for axonal sorting into glomeruli in the mouse olfactory system. Cell *117*, 817–831.

Fishilevich, E., and Vosshall, L.B. (2005). Genetic and functional subdivision of the *Drosophila* antennal lobe. Curr. Biol. *15*, 1548–1553.

Galizia, C.G., Sachse, S., Rappert, A., and Menzel, R. (1999). The glomerular code for odor representation is species specific in the honeybee *Apis mellifera*. Nat. Neurosci. *2*, 473–478.

Gogos, J.A., Osborne, J., Nemes, A., Mendelsohn, M., and Axel, R. (2000). Genetic ablation and restoration of the olfactory topographic map. Cell *103*, 609–620.

Hallem, E.A., and Carlson, J.R. (2006). Coding of odors by a receptor repertoire. Cell *125*, 143–160.

Hallem, E.A., Ho, M.G., and Carlson, J.R. (2004). The molecular basis of odor coding in the *Drosophila* antenna. Cell *117*, 965–979.

Hickmott, P.W., and Steen, P.A. (2005). Large-scale changes in dendritic structure during reorganization of adult somatosensory cortex. Nat. Neurosci. *8*, 140–142.

Hubel, D.H., and Wiesel, T.N. (1962). Receptive fields, binocular interaction and functional architecture in the cat's visual cortex. J. Physiol. *160*, 106–154.

Hummel, T., and Zipursky, S.L. (2004). Afferent induction of olfactory glomeruli requires N-cadherin. Neuron *42*, 77–88.

Hummel, T., Vasconcelos, M.L., Clemens, J.C., Fishilevich, Y., Vosshall, L.B., and Zipursky, S.L. (2003). Axonal targeting of olfactory receptor neurons in *Drosophila* is controlled by *Dscam*. Neuron *37*, 221–231.

Imai, T., Suzuki, M., and Sakano, H. (2006). Odorant receptor-derived cAMP signals direct axonal targeting. Science *314*, 657–661.

Johnson, B.A., Woo, C.C., and Leon, M. (1998). Spatial coding of odorant features in the glomerular layer of the rat olfactory bulb. J. Comp. Neurol. *393*, 457–471.

Jones, W.D., Cayirlioglu, P., Kadow, I.G., and Vosshall, L.B. (2007). Two chemosensory receptors together mediate carbon dioxide detection in *Drosophila*. Nature *445*, 86–90.

Kano, M., Rexhausen, U., Dreessen, J., and Konnerth, A. (1992). Synaptic excitation produces a long-lasting rebound potentiation of inhibitory synaptic signals in cerebellar Purkinje cells. Nature *356*, 601–604.

Katz, L.C., and Shatz, C.J. (1996). Synaptic activity and the construction of cortical circuits. Science *274*, 1133–1138.

Keene, A.C., Stratmann, M., Keller, A., Perrat, P.N., Vosshall, L.B., and Waddell, S. (2004). Diverse odor-conditioned memories require uniquely timed dorsal paired medial neuron output. Neuron *44*, 521–533.

Keller, A., and Vosshall, L.B. (2007). Influence of odorant receptor repertoire on odor perception in humans and fruit flies. Proc. Natl. Acad. Sci. USA *104*, 5614–5619.

Komiyama, T., Carlson, J.R., and Luo, L. (2004). Olfactory receptor neuron axon targeting: intrinsic transcriptional control and hierarchical interactions. Nat. Neurosci. *7*, 819–825.

Kwon, J.Y., Dahanukar, A., Weiss, L.A., and Carlson, J.R. (2007). The molecular basis of CO_2 reception in *Drosophila*. Proc. Natl. Acad. Sci. USA *104*, 3574–3578.

Laissue, P.P., Reiter, C., Hiesinger, P.R., Halter, S., Fischbach, K.F., and Stocker, R.F. (1999). Three-dimensional reconstruction of the antennal lobe in *Drosophila melanogaster*. J. Comp. Neurol. *405*, 543–552.

Larsson, M.C., Domingos, A.I., Jones, W.D., Chiappe, M.E., Amrein, H., and Vosshall, L.B. (2004). *Or83b* encodes a broadly expressed odorant receptor essential for *Drosophila* olfaction. Neuron *43*, 703–714.

Lei, H., Christensen, T.A., and Hildebrand, J.G. (2002). Local inhibition modulates odor-evoked synchronization of glomerulus-specific output neurons. Nat. Neurosci. *5*, 557–565.

Liu, S.J., and Lachamp, P. (2006). The activation of excitatory glutamate receptors evokes a long-lasting increase in the release of GABA from cerebellar stellate cells. J. Neurosci. *26*, 9332–9339.

Lin, D.Y., Shea, S.D., and Katz, L.C. (2006). Representation of natural stimuli in the rodent main olfactory bulb. Neuron *50*, 937–949.

Malnic, B., Hirono, J., Sato, T., and Buck, L.B. (1999). Combinatorial receptor codes for odors. Cell *96*, 713–723.

Mizrahi, A., and Katz, L.C. (2003). Dendritic stability in the adult olfactory bulb. Nat. Neurosci. *6*, 1201–1207.

Mombaerts, P., Wang, F., Dulac, C., Chao, S.K., Nemes, A., Mendelsohn, M., Edmondson, J., and Axel, R. (1996). Visualizing an olfactory sensory map. Cell *87*, 675–686.

Nakai, J., Ohkura, M., and Imoto, K. (2001). A high signal-to-noise Ca^{2+} probe composed of a single green fluorescent protein. Nat. Biotechnol. *19*, 137–141.

Ng, M., Roorda, R.D., Lima, S.Q., Zemelman, B.V., Morcillo, P., and Miesenbock, G. (2002). Transmission of olfactory information between three populations of neurons in the antennal lobe of the fly. Neuron *36*, 463–474.

Olsen, S.R., Bhandawat, V., and Wilson, R.I. (2007). Excitatory interactions between olfactory processing channels in the *Drosophila* antennal lobe. Neuron *54*, 89–103.

Pelz, D., Roeske, T., Syed, Z., de Bruyne, M., and Galizia, C.G. (2006). The molecular receptive range of an olfactory receptor in vivo (*Drosophila melanogaster Or22a*). J. Neurobiol. *66*, 1544–1563.

Ressler, K.J., Sullivan, S.L., and Buck, L.B. (1994). Information coding in the olfactory system: evidence for a stereotyped and highly organized epitope map in the olfactory bulb. Cell *79*, 1245–1255.

Sachse, S., and Galizia, C.G. (2002). Role of inhibition for temporal and spatial odor representation in olfactory output neurons: A calcium imaging study. J. Neurophysiol. *87*, 1106–1117.

Scott, K., Brady, R., Jr., Cravchik, A., Morozov, P., Rzhetsky, A., Zuker, C., and Axel, R. (2001). A chemosensory gene family encoding candidate gustatory and olfactory receptors in *Drosophila*. Cell *104*, 661–673.

Shang, Y., Claridge-Chang, A., Sjulson, L., Pypaert, M., and Miesenbock, G. (2007). Excitatory local circuits and their implications for olfactory processing in the fly antennal lobe. Cell *128*, 601–612.

Stortkuhl, K.F., and Kettler, R. (2001). Functional analysis of an olfactory receptor in *Drosophila melanogaster*. Proc. Natl. Acad. Sci. USA *98*, 9381–9385.

Suh, G.S., Wong, A.M., Hergarden, A.C., Wang, J.W., Simon, A.F., Benzer, S., Axel, R., and Anderson, D.J. (2004). A single population of olfactory sensory neurons mediates an innate avoidance behaviour in *Drosophila*. Nature *431*, 854–859.

Tanaka, N.K., Awasaki, T., Shimada, T., and Ito, K. (2004). Integration of chemosensory pathways in the *Drosophila* second-order olfactory centers. Curr. Biol. *14*, 449–457.

Vassar, R., Chao, S.K., Sitcheran, R., Nunez, J.M., Vosshall, L.B., and Axel, R. (1994). Topographic organization of sensory projections to the olfactory bulb. Cell *79*, 981–991.

Vosshall, L.B., and Stocker, R.F. (2007). Molecular architecture of smell and taste in *Drosophila*. Annu. Rev. Neurosci. *30*, 505–533.

Vosshall, L.B., Wong, A.M., and Axel, R. (2000). An olfactory sensory map in the fly brain. Cell *102*, 147–159.

Wang, J.W., Wong, A.M., Flores, J., Vosshall, L.B., and Axel, R. (2003). Two-photon calcium imaging reveals an odor-evoked map of activity in the fly brain. Cell *112*, 271–282.

Wilson, R.I., and Laurent, G. (2005). Role of GABAergic inhibition in shaping odor-evoked spatiotemporal patterns in the *Drosophila* antennal lobe. J. Neurosci. *25*, 9069–9079.

Wilson, R.I., Turner, G.C., and Laurent, G. (2004). Transformation of olfactory representations in the *Drosophila* antennal lobe. Science *303*, 366–370.

Winnington, A.P., Napper, R.M., and Mercer, A.R. (1996). Structural plasticity of identified glomeruli in the antennal lobes of the adult worker honey bee. J. Comp. Neurol. *365*, 479–490.

Wong, A.M., Wang, J.W., and Axel, R. (2002). Spatial representation of the glomerular map in the *Drosophila* protocerebrum. Cell *109*, 229–241.

Yu, D., Ponomarev, A., and Davis, R.L. (2004). Altered representation of the spatial code for odors after olfactory classical conditioning; memory trace formation by synaptic recruitment. Neuron *42*, 437–449.

Zhu, H., and Luo, L. (2004). Diverse functions of N-cadherin in dendritic and axonal terminal arborization of olfactory projection neurons. Neuron *42*, 63–75.

Zhu, H., Hummel, T., Clemens, J.C., Berdnik, D., Zipursky, S.L., and Luo, L. (2006). Dendritic patterning by Dscam and synaptic partner matching in the *Drosophila* antennal lobe. Nat. Neurosci. *9*, 349–355.